

Dear reviewer,

Thank you very much for your valuable remarks, comments and suggestions. We find that by answering your questions and comments, and by following your suggestions, we have improved the readability of our work.

We start by answering the points raised in your general comment and then proceed with the section-specific suggestions/corrections.

In this document, your original comments are framed by a box and our answer follows.

Answer to the general comment:

First, you improve the performances of your previous work (Caseiro et al 2018) in detecting flaring sites, adding a temperature filtering.

We indeed complete our previous work with a filtering procedure which is based on the analysis of the temperature time series retrieved at the location of a given detection (the maximum temperature must be larger than 1500K) and on the persistence of the signal at that location (more than 5 quality detections per year).

When you compare your results with VNF, you first use the 2012 VNF outputs (why not the 2017?) and then you take into account the combustion sources (https://ngdc.noaa.gov/eog/viirs/download_viirs_fire.html) identified by VNF instead of the flaring sites available at https://www.ngdc.noaa.gov/eog/viirs/download_global_flare.html for 2017 (the year of your analysis). I think it is a forcing applying the criteria developed in this work for SLSTR to select among the VNF combustion sources the flaring sites. The latter are directly provided by NOAA at https://www.ngdc.noaa.gov/eog/viirs/download_global_flare.html.

Our first decision was to use only published data for the activity and emissions comparisons and the most up-to-date VNF data for the characterisation (in our case, temperature), after applying a similar procedure as the one used in our work (i.e. gridding). We accept the suggestion and include the 2017 VNF temperature and activity data in our analysis. See section 3.5 for the comparison with the 2017 VNF dataset.

We now answer the section-specific suggestions/corrections:

Abstract

- We calculate the global flared gas volumes and black carbon emissions in 2017 by ~~(1)~~ applying (1) a previously developed hot spot detection and characterisation algorithm to all observations of the SLSTR instrument on-board the Copernicus 5 satellite Sentinel-3A ~~in 2017~~ and (2) ~~applying~~ newly developed filters for identifying gas flares and corrections for calculating both flared gas volumes (BCM) and black carbon emission (g/m^3) estimates.
- The comparison of our results with those of the VIIRS Nightfire data set indicates a good fit between the two methods.
- Please, remove the space at the beginning of the bracket (<https://eccad3.sedoo.fr/#GFlaringS3>, DOI 10.25326/19 (Caseiro and Kaiser, 2019))

All your recommendations were followed in the updated manuscript, except the units for the BC emissions, which we kept as mass (g).

Introduction

- Please, put the dot after the references: or convert the gas; (Rahimpour and Jokar, 2012; Emeka Ojijiagwo et al., 2016). This is the first case, I found many others in the paper.
- Improvements of flare gas recovery systems have been recommended ...
- GF also impacts the environment on a wider scale through the emission of pollutants and greenhouse gases like carbon dioxide (CO_2), carbon monoxide, black carbon (BC)...
- Of particular importance is also the black carbon (BC) emission emitted by GF. BC is a known carcinogen (Heinrich et al., 1994) as well as a short-lived climate forcer (IPCC, 2013). BC strongly affects environments such ...
- Satellite remote sensing has been utilized for regional and global identification and characterization of GF- (Casadio et al., 2012b, a; Anejionu et al., 2014; Faruolo et al., 2014; Chowdhury et al., 2014; Anejionu et al., 2015; Faruolo et al., 2018). The most prominent system is NOAA's VIIRS (here add NOAA acronym Visible Infrared Imaging Radiometer Suite) Nightfire (VNF) dataset (see https://ngdc.noaa.gov/eog/viirs/download_viirs_fire.html), developed by Elvidge et al. (2013, 2016) for the detection and characterization of combustion sources based on previous work (Elvidge et al., 2001, 2007, 2009, 2013) and leading to a globally consistent survey of gas flaring volumes available extending back to 2012 (https://www.ngdc.noaa.gov/eog/viirs/download_global_flare.html).
- We recently published an adaptation and extension of the VNF-VIIRS Nightfire algorithm with which observations of the SLSTR instrument (Sea and Land Surface Temperature Radiometer) instrument on-board the Sentinel-3A satellites have been analysed, too (Caseiro 30 et al., 2018).

- [last comment in the above box] Since the methodology is applicable to all (to date 2) the SLSTR instruments, we prefer to keep the reference to the Sentinel-3 satellites in the plural.
- All the other recommendations were followed in the updated manuscript.

- The main advantages of using our hot spot detection and characterisation algorithm lie in the ability to detect and quantify smaller flares and the foreseen long term data availability from the series of Sentinel-3 satellites in the Copernicus program. Additionally, SLSTR observations (night-time overpasses at 10:00 PM) complement those of VIIRS (1:30 AM) by filling observation gaps in the time series. I think the unique advantage your algorithm seems to offer, when compared to VNF, is its capability to identify smaller flares. Regarding the data continuity, also VIIRS is actually onboard two satellites (Suomi NPP and JPSS-1) and will also be flown on the JPSS-2 (launch in 2021), -3 (2026) and -4 (2031) satellite missions. You can rephrase this sentence, pointing out the potential of these algorithms, the possibility of integrating them as well as of continuously monitoring the phenomenon thanks to the long design life of satellite missions.
- Here, we describe a new dataset of global gas flaring volumes (BCDM) and BC emissions (g/m^3), which we have derived from all Sentinel-3A SLSTR observations in 2017. In detail, Chapter 2 describes newly developed methods for identifying gas flares among the observed hot sources, correcting for intermittent observations opportunities, and dynamically determining appropriate BC emission factors from the observations. The results of applying the hot source detection and characterisation algorithm plus the newly developed methods to all SLSTR observations of 2017 are presented in Chapter 3, the Finally, our conclusions are summarised in Chapter 4.
- While in principle the methodology used is based on the Nightfire algorithm developed for VIIRSVNF
- We already tested the method using oil and/or gas producing regions within a limited timespan and compared the results to the VNF-VIIRS Nightfire

All your recommendations were followed in the updated manuscript, except the units for the BC emissions, which we kept as mass (g). Regarding the first comment of the box above, we have rephrased the idea focusing the complementarity of the instruments and the methods.

2.1 Hot spot detection and characterization

Figure 1 should be improved, explaining the GF filter.

2.2 Hot spot classification

2.2.1 Volcano filter

- The data ~~were~~ filtered
- Many volcanoes do not consist of a single edifice, ~~but a volcanic field with~~ many individual eruptive fissures through which lava erupts ~~may be present in a volcanic field~~. (Siebert et al., 2010).

We have updated the manuscript following all these recommendations.

2.2.2 Discrimination of gas flares from other industrial hot sources

This paragraph is not completely clear. You are searching for a criterion to use for accurately detecting flaring sites. The starting point is your algorithm (Caseiro et al., 2018), to which you add a temperature filtering. I do not understand how you use the works of Elvidge et al. (2016) and Liu et al. (2018) in the definition of the temperature criterion. To this aim, you test several subsets. Can you explain what are these subsets? They are 8? They correspond the 8 columns in Table 1? Besides, I expected n_{Obs} was greater than n_{ObsHA} . Probably, it is more correct to use \geq than $>$.

We have updated the caption of Table 1 with more detail:

Table 1. User's accuracy (UA, %) and commission error (C, %) of the hot spot discrimination strategies considered. n_{Obs} is the number of hot spot detections within a grid cell, n_{ObsHA} is the number of high-accuracy hot spot detections within a grid cell, T_{min} is the minimum temperature retrieved among all the hot spots detected within a grid cell, T_{max} is the maximum temperature retrieved among all the hot spots detected within a grid cell, n_{cells} is the number of grid cells that comply to the thresholds. In order to discriminate gas flares from other hot spots we discriminate hot spots based on their persistency (n_{Obs} and n_{ObsHA}) and on their temperature time series (T_{min} and T_{max}). We have tried 8 combinations (discrimination strategies) of thresholds on those variables. Each column represent a tested discrimination strategy. For each of the 8 combinations, we examine high-resolution imagery for 100 random onshore locations (800 in total) in order to verify the presence of a gas flare. The goal is to maximize user's accuracy (UA) and minimize commission error (C) while minimizing the omission error (here, the variation in n_{cells} is used as a proxy). The discrimination strategy #5 was selected as the most suitable.

| combination | #1 | #2 | #3 | #4 | #5 | #6 | #7 | #8 |
|-----------------|------|------|-------|-------|-------|-------|-------|-------|
| $n_{Obs} >$ | - | 3 | 4 | - | - | - | - | - |
| $n_{ObsHA} >$ | 2 | 2 | 2 | 5 | 5 | 5 | 7 | 7 |
| $T_{min} (K) >$ | 1000 | 1000 | - | - | - | - | - | - |
| $T_{max} (K) >$ | 1400 | 1400 | 800 | 1200 | 1500 | 1800 | 1200 | 1500 |
| n_{cells} | 6733 | 5872 | 9469 | 6817 | 6232 | 5485 | 5527 | 5129 |
| UA | 84±6 | 86±8 | 60±10 | 77±13 | 85±11 | 88±10 | 73±14 | 87±11 |
| C | 7±3 | 4±2 | 19±11 | 6±4 | 3±1 | 1±1 | 8±5 | 2±1 |

In the text, we also give more detail in order to explain how we based our temperature considerations on the works of C. Elvidge and Y. Liu:

The temperature value used in the selection process of a discrimination strategy is based on Elvidge et al. (2016) and on the recent work by Liu et al. (2018), who derived gas flaring temperatures of 1000 K to 2600 K from the VIIRS Nightfire database, depending on the type of operation (shale oil or gas, offshore, onshore or refinery). Most of the gas flares display temperatures between 1650 K and 1850 K. However, temperatures can occasionally be as low as 1300 K. We therefore test for the minimum and/or for the maximum temperature for all the high-accuracy detections within a grid cell (T_{min} and T_{max} , respectively). The temperature range reported by Elvidge et al. (2016) and Liu et al. (2018) overlaps with particularly hot detections from the coal chemical industry and steel plants. Therefore, additional criteria are needed for identifying gas flares in the hot source dataset.

In order to select the discriminating strategy we test several subsets of the gridded high-accuracy hot spot database. For each of the 8 subsets described in Table 1, a sample of 100 random onshore grid cells complying to the defined thresholds have been tested by examining high-resolution imagery (Google Earth) and the locations are classified into four categories:

2.3 Determination of flared volumes and black carbon emissions

- Please, explain the terms BCMmin, BCMmax, BCMbest in this order, to facilitate the comprehension.

This was updated as suggested.

- The emissions of black carbon (BC) from gas flares are estimated using reported emissions factors (EF). It could be useful to specify the formulation applied for their computation.

We have somewhat rearranged this paragraph and included a short introductory text to explain our approach:

The emissions of black carbon (BC) from gas flares are estimated using reported emissions factors (EF). Klimont et al. (2017) recognized the limited number of measurements of flaring emissions. Here, we attempt to consider the limited information available on the EF and maximize the use of the available information on the flare characteristics.

Schwarz et al. (2015) and Weyant et al. (2016) conducted field experiments in the Bakken formation (USA) and derived EFs of $0.57 \pm 0.14 \text{ g.m}^{-3}$ and $0.13 \pm 0.36 \text{ g.m}^{-3}$ (using the Single Particle Soot Photometer) or 0.28 g.m^{-3} (using the Particle Soot Absorption Photometer), respectively. However, flared gas has not the same composition everywhere and Huang and Fu (2016) considered the regional variability of the EF. The authors applied the function which relates EF to the volumetric gas heating value derived in the laboratory by McEwen and Johnson (2012) to globally compiled gas composition data. Klimont et al. (2017) considered, for the Greenhouse Gas – Air Pollution Interactions and Synergies (GAINS) model, the EF derived by Schwarz et al. (2015) of 0.57 g.m^{-3} for well-operated flares (i.e. Organisation for Economic Co-operation and Development (OECD) countries) and a maximum of 1.75 g.m^{-3} for other countries. Stohl et al. (2013) used an EF of 1.6 g.m^{-3} from a previous GAINS version. In the present work, we apply the same concept of a varying EF but use the flare temperature as an indication of the combustion completeness, instead of the country of origin as an indication of the flare operation. Flaring temperatures close to the adiabatic flame temperature for natural gas (around 2500 K) are associated with more complete combustion and therefore lower BC emissions. On the other hand, low flaring temperatures (700 K and below) are associated with higher BC emissions. Between the two extremes, the BC emission is scaled linearly as a function of the flaring temperature (see Figure 3). To the best of our knowledge, this is the first time that operating practices are taken into consideration when assigning the EF.

- GAINS: please, extend the acronym.

The acronym is explained in the text.

- You define flaring site a site with a temperature above 1500K. Why do you compute the EFs for lower temperatures?

The flaring site is defined as a grid cell for which the count of high-accuracy hot spots is larger than 5 and the maximum temperature is larger than 1500K. Although the maximum retrieved temperature must be larger than 1500K, temperature for individual high-accuracy hot spots within the grid cell may be lower than 1500K.

- With this methodology we estimate a wide range of possible activity (BCM) and BC emissions (g/m^3)

The recommendation was followed in the updated manuscript although the unit for the BC emissions was kept as mass (g).

- Can you better explain this sentence, please? I do not understand it: "We conservatively assume that this range of possibilities represents $6 \times \sigma$, and report the uncertainty of the best estimates as $1 \times \sigma$ ".

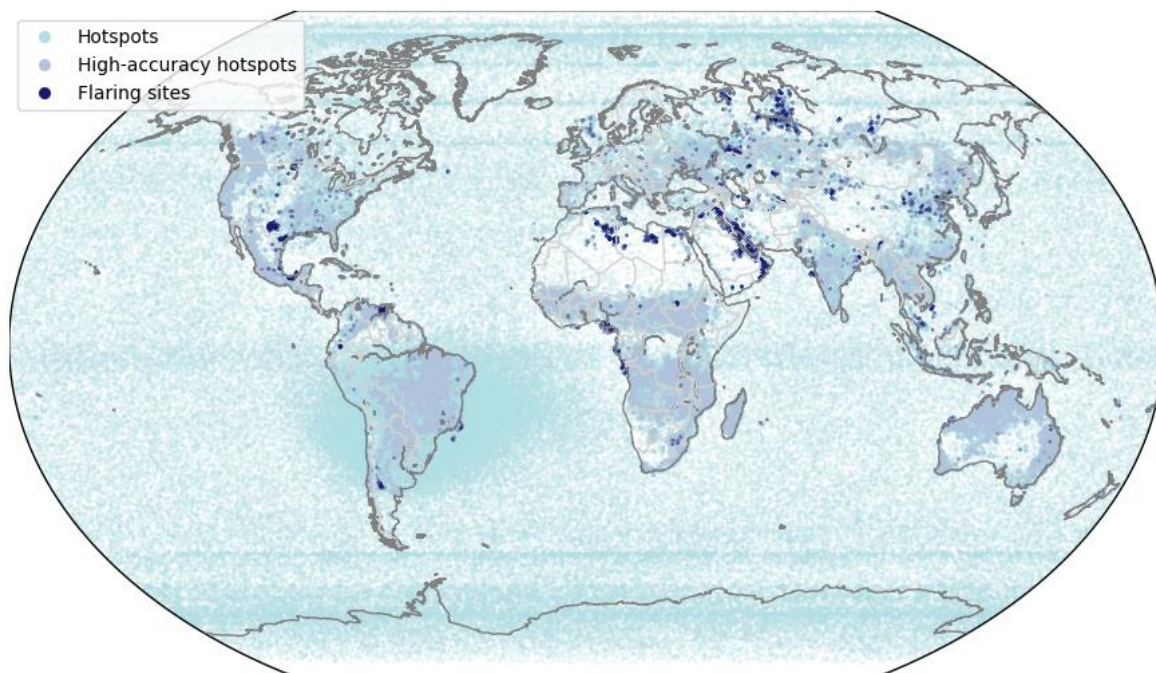
For clarity, we have removed this part from the paper and report the best estimate together with the range.

3. Results

3.1 Hot spots and flaring sites

I have concerns about this section. Your paper focuses on gas flaring, the previous one (Caseiro et al., 2018) on hotspots. For this reason, you can join Figures 4, 5, 6 using three colors for discriminating hotspots, high confidence hotspots and flaring sites. Besides, I do not understand why you compare the SLSTR global detections for 2017 with the VNF in 2012. The VNF data for 2017 are available; you indeed use them in section 3.3.

Figures 4, 5 and 6 were merged into a single figure. Please see the resulting figure below.



- Russia (985) and the United States (917) are the countries with the highest number of flaring locations (Figure 7).
- The time series of the cumulative number of the high accuracy observations for the most active flaring location (in Venezuela, see Section 3.4) is shown in Figure 8. It shows flaring activity throughout the year. In my opinion, it is not useful and interesting. Remove Figure 8.

These suggestions were followed.

I think 3.2 and 3.3 are subsections of 3.1: they become 3.1.1 and 3.1.2.

We feel that the three sections bring enough information individually to be treated as being at the same level: 3.1 deals with the detection itself, 3.2 with their characteristics and in 3.3 we derive the activity. To make this clear, the title of 3.1 has been updated: "Flaring locations".

- Figures 10, 11 and 12 are not useful, in my opinion they could be removed. You can indeed add before Figure 9 and Figure 13, respectively, a global map (in color scale) showing the temperatures and RP values for the 6232 sites.

We have removed Figures 10, 11 and 12.

We have added figures for the global average T distribution:

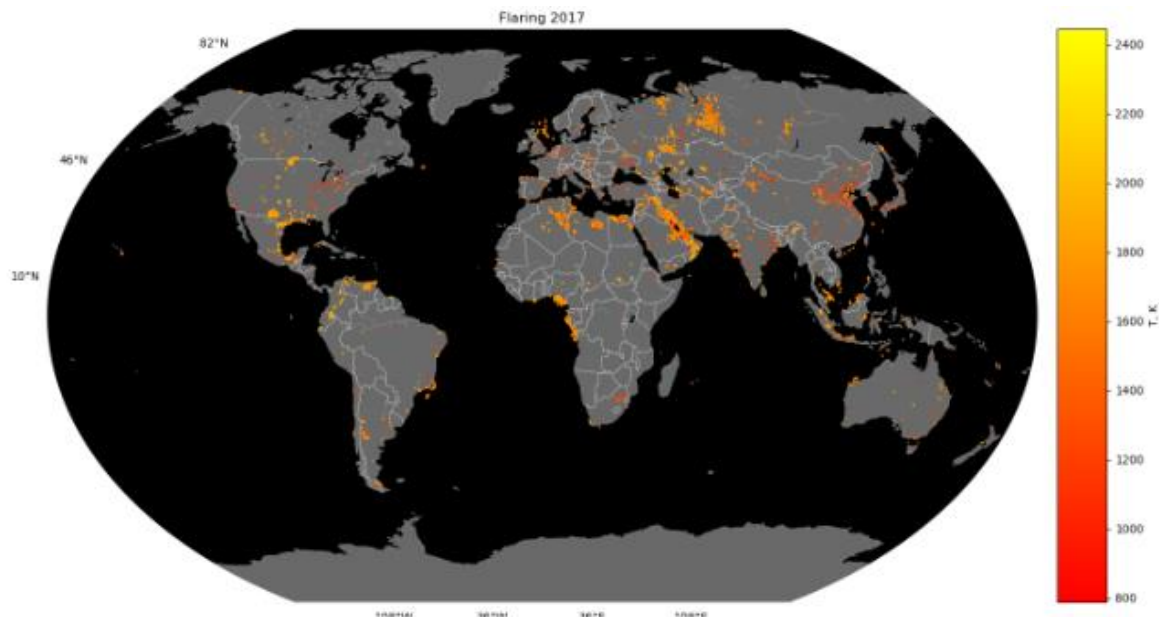


Figure 7. Average flaring temperature (K) at the 6232 flaring locations.

and similarly for RP:

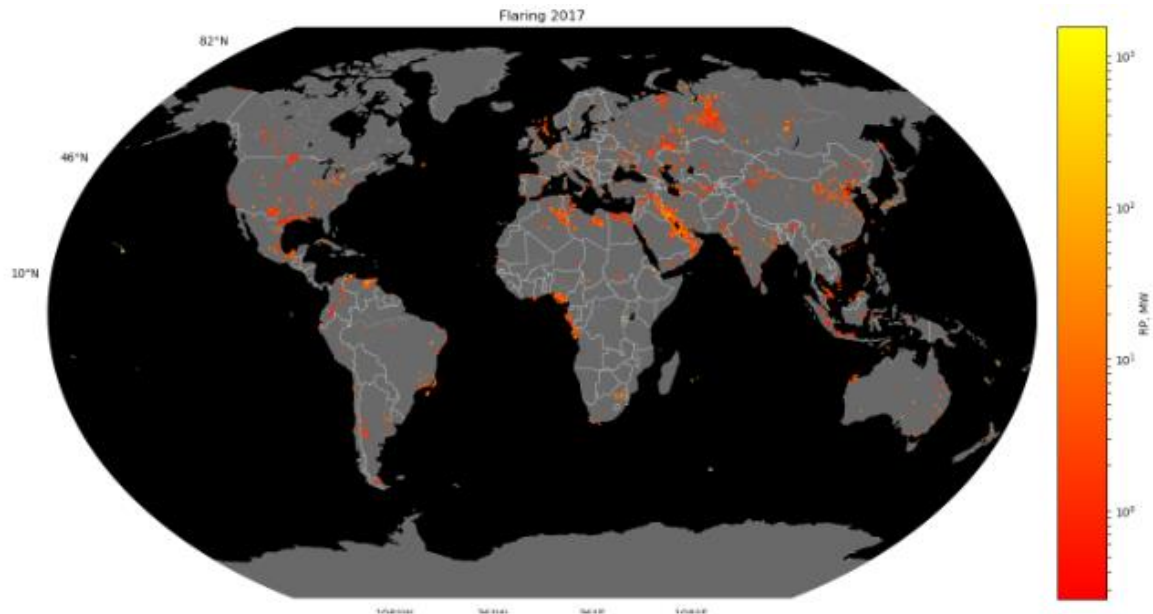


Figure 9. Average radiative power (MW) at the 6232 flaring locations.

- Figure 9. Distribution of the average retrieved **hot-spot** temperature (K) for the flaring locations

The suggestion was followed.

- The average temperature at the flaring locations approximately ranges from 950 K to 2250 K. This is slightly lower than the range reported by Liu et al. (2018) ([please, can you specify the values](#)) who used VIIRS Nightfire data, as expected from our previous study (Caseiro et al., 2018). It confirms the bi-modal distribution with modes around 1750 K and 1200 K that is has also been observed by VIIRS.

The range given in Liu et al. (2018) was specified in the manuscript.

- The section "Comparison with VIIRS Nightfire" should be modified. As before explained, being the focus of your work the gas flaring, you should compare your results with the VNF flaring sites (available at https://www.ngdc.noaa.gov/eog/viirs/download_global_flare.html), avoiding to select these sites among the VNF combustion sources applying the criteria used for SLSTR.

The section was rewritten taking into consideration your suggestions. The section is now at the end of the "Results" chapter and we included a comparison of the activity (flared volumes) as well.

- You never cite Figure 14 in the paper. The figure is not useful, as figures 10-12.

Figure 14 was removed from the manuscript.

3.4 Flared volumes [\(new 3.2\)](#)

As before, you should use BCM data available at https://www.ngdc.noaa.gov/eog/viirs/download_global_flare.html for the comparison with your estimates in 2017. It would be interesting the map of the global distribution of BCMbest. In Figure 20 you could add the distribution derived by the VNF data elaboration.

3.5 BC emissions [\(new 3.3\)](#)

As for BCM, you can add a global map of BC emissions.

This section was reworked also following the recommendations from the other reviewer and the short comments. It now includes VNF data from 2017 as suggested. Please see the updated manuscript.

Conclusions

To reorganize based on new suggested analyses. In any case:

This section was reworked also following the recommendations from the other reviewer and the short comments. Please see the updated manuscript.

- The sentence “We present a new gas flaring discrimination procedure, based on two characteristics of gas flares: persistence and temperature” is not correct. This procedure is not new, being the one most used to identify gas flares. Respect to your methodology, you simply add a temperature filtering to improve the detection of flaring sites.

We have updated this sentence of the conclusions: “We adapt the procedure most commonly used to discriminate gas flares (based on two characteristics of gas flares: persistence and temperature) to our specific hotspot detection methodology.”

- “Additionally to the detection we present a way to assess the volume of flared gas”: is not true. You apply a widely declared model developed by Elvidge et al (2016) to compute monthly flared volumes, adding a scaling factor, which takes into account the operation time of the sites.

We have reworded the first two sentences of this paragraph: “Additionally to the detection we assess the volume of flared gas based on the observed relationship between the flared volume and observed flare radiative energy.”